Journal of Spatial Information Sciences

... JSIS

ANALYSIS OF THE IMPACT OF LAND USE AND LAND COVER TYPES ON LAND SURFACE TEMPERATURE OF IMO STATE, NIGERIA

Ukanwa, S. O., Ejikeme, J. O and Aweh, D.S

JOURNAL OF SPATIAL INFORMATION SCIENCES
VOL1, ISSUE 1, PP 74–89, 2024
PUBLISHED 10-10-2024

www.journals.unizik.edu.ng/jsis

ANALYSIS OF THE IMPACT OF LAND USE AND LAND COVER TYPES ON LAND SURFACE TEMPERATURE OF IMO STATE, NIGERIA

[1]Ukanwa, S. O., [1]Ejikeme, J. O., and [1]Aweh, D. S.

[1]Department of Surveying and Geoinformatics, Nnamdi Azikiwe University, Awka, Anambra State

ABSTRACT

The uncontrolled rapid urban expansion and landuse/landcover transformations alters the hydrological, thermodynamic, and radioactive activities of the earth surface, and this amplifies the effects of climate change and heat waves. This study was aimed at performing a spatiotemporal analysis of land surface temperature and its impact on land use/land cover types in Imo State of Nigeria. Lansat 8 OLI imageries of 2013, 2018 and 2023 were used for data analysis to retrieve the land surface temperature (LST) and the land use/ land cover (LULC) types. The methodology adopted by study for LST retrieval was the Single Channel Algorithm (SCA) and for classifying the LULC, the Supervised Classification using Maximum Likelihood Classifier (MLC) algorithm was used. The ArcGIS 10.8 was used to classify LULC types and estimate the LST. The findings suggest that because of the biophysical properties of the land surfaces, LULC has a considerable impact on LST values.. The greatest LST variations were found between water bodies and vegetation, but moderate LST differences were found between bare lands and vegetation as well as between barren land and built-up regions. The study also revealed that the highest LSTs occur in the state's capital Owerri and also Mgbidi Town. The study will have a positive health impact in the study area and help policies makers and relevant agencies in making an information decision and policies based on the findings from the study.

KEYWORDS: ***Land Use/Land Cover (LULC) classification*****, LST, SCA and SCA**

1. Introduction

In urban areas, landuse/ landcover changes are a critical factor affecting the physical characteristics of the Earth's surface due to the unique characteristics that each landuse and landcover (LULC) category possesses with respect to radiation and absorption of energy on the Earth's surface (Koko *et al.*, 2021).These changes affect the degree of absorption of solar radiation, albedo, surface temperature, evaporation rates, transmission of heat to the soil, storage of heat, wind turbulence, can drastically alter the conditions of the near-surface atmosphere over the cities (Mallick*et al.*, 2008), modify energy and water balance processes as well as playing a vital role in many environmental processes (Weng*et al.*, 2004). The land surface temperature can be considered an effective measure for predicting radiation budgets for heat balance, it can be an important indicator in understanding the interactions that occur between the environment and humans in urban environments and also an important factor controlling the physical and biological processes of land systems (Tan *et al*., 2010). Furthermore, the increase in land surface temperature effects the urban heat island (UHI) phenomena, having a significant influence on biodiversity's primary function, local and regional climate (Luck and Wu, 2002).

As a result of the spatiotemporal landuse/ landcover variations, this alters on the pattern of a variety of land surfaces of spatial landscapes and it is therefore critical to ascertain landuse/ landcover changes at appropriate scales using accurate time series data. Studies have shown that land cover changes influence the surface temperature due to the different heat capacity of soils associated to a given amount of solar radiation (Fonseka*et al*., 2019).

Anambra State, located in southeastern Nigeria, has experienced considerable LULC changes over the past few decades. This study aims to analyze the spatiotemporal dynamics of these changes and assess their impacts on land surface temperature (LST), a critical parameter influencing local climate and environmental conditions.

2.Materials and Methods

2.1 Study Area

Imo State is located in the southeastern region of Nigeria and is one of the 36 states in the country. The state lies within latitudes 4°45'N and 7°15'N, and longitude 6°50'E and 7°25'E, with an area

of around 5,100 sq km. Imo State is bordered by Anambra State to the north for 84 km (52 miles), Abia State to the east for about 104 km (partly in the vicinity of the Imo River), and Rivers State to the south and west for about 122 km.In Imo State,the rainy season begins in April and lasts until October, with annual rainfall varying from 1,500 mm to 2,200 mm (60 to 80 inches).An average annual temperature above 20 °C (68.0 °F), creates an annual relative humidity of 75%. With humidity reaching 90% in the rainy season.The state has a high population density, reflecting its relatively small geographic size compared to its large population.

Fig. 1 shows the map of the study area.

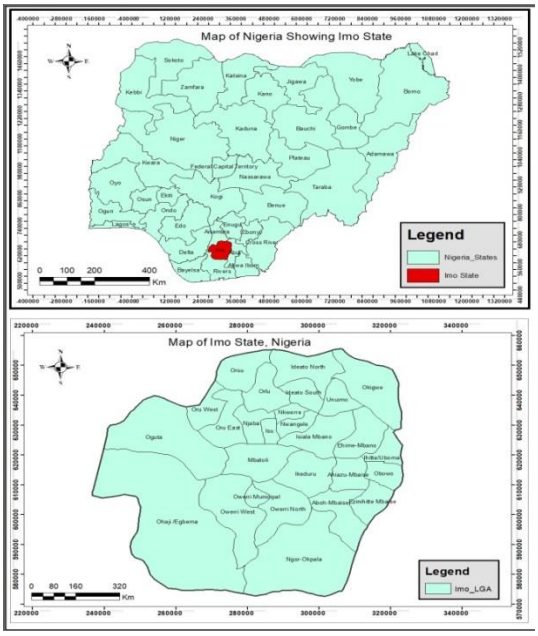

Fig 1: Map of the study area

2.2 Materials

Table 1.shows the different datasets used for this study and their sources.

S/N	Data	Acquisition Date	Scale	Source

1	Landsat 8 OLI_TIRS	2013-04-14	30m ™	U.S. Geological Survey(USGS)
2	Landsat 8 OLI_TIRS	2018-06-26	30m ™	U.S. Geological Survey(USGS)
3	Landsat 8 OLI_TIRS	2023-07-01	30m ™	U.S. Geological Survey (USGS)
4	Google Earth Data			Google Earth
5	Administrative Map of Imo State			OSGOF

2.3 Methods

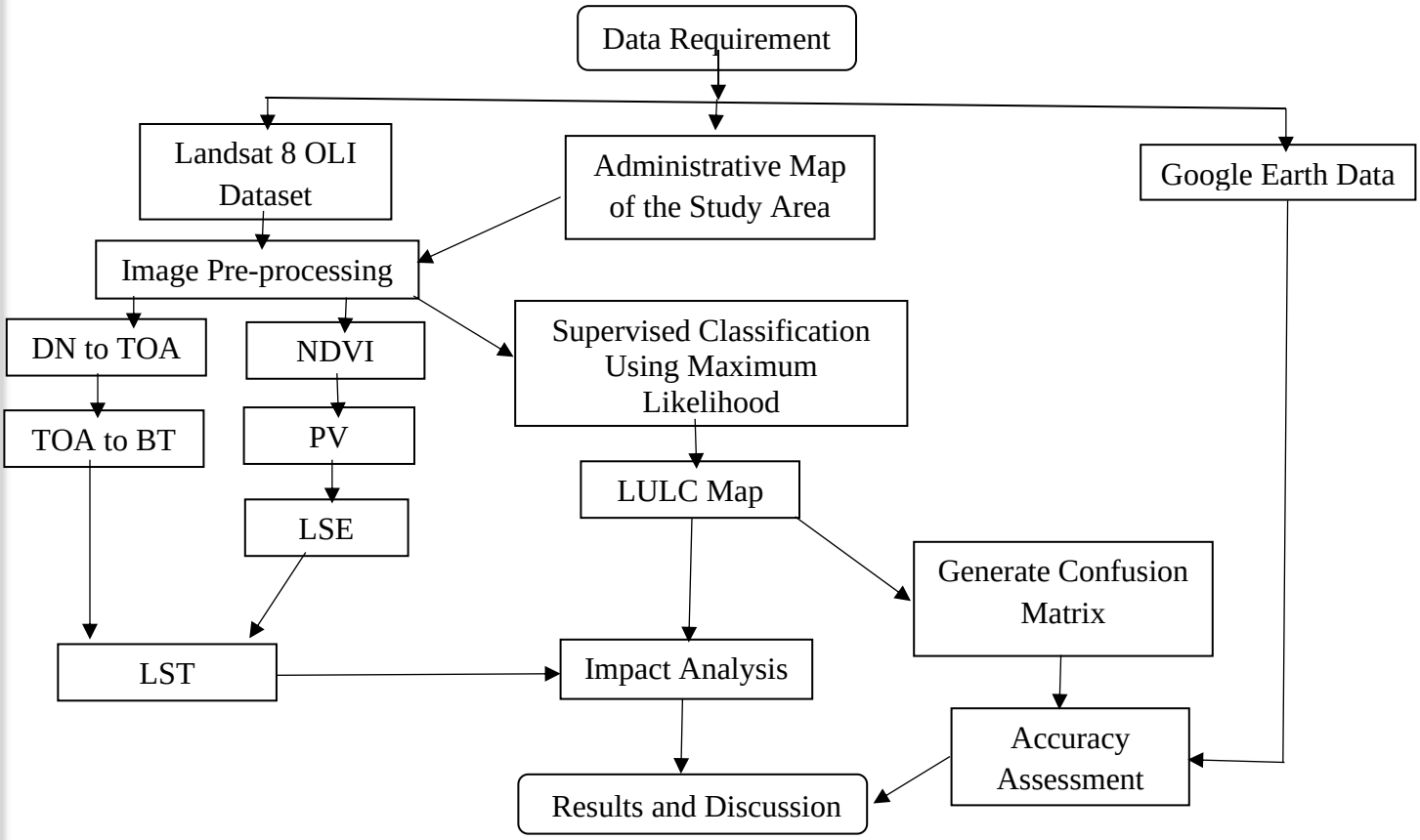

Fig 2: Flowchart of methodology adopted by the study

Source: The Author

2.4 Image Processing and Classification

The supervised classification approach was used to the Landsat 8 OLI imageries for LULC categorization. The training samples for the supervised classification operation were made using

the previous information of the research region. Using polygons drawn in an area of interest (AoI) layer in the satellite images, training samples were produced. The supervised classification classifier was the maximum likelihood algorithm, and the signature file was generated. Over the years, medium-resolution satellite data, such as that obtained from Landsat 8 OLI, has been classified extensively using the maximum likelihood classifier (MLC).The maximum likelihood classifier uses a statistical method to identify patterns, and it makes the assumption that each class's statistics in each image band have a normal distribution. The algorithm's implementation is straightforward and extensively utilized for diverse remote sensing applications. It calculates the likelihood that a particular pixel belongs to each class and designates it accordingly (Ahmad and Quegan, 2012).

Table 2.0 shows the different land use and land cover types for the study.

Table 2: Description of land cover types for the study.

S/N	LULC Category	Description
1.	Built-up lands	All residential, commercial, and industrial areas, village settlements, and transportation infrastructure
2	Vegetation covers	Trees, shrub land and semi-mature vegetation, deciduous, coniferous, and mixed forests, palms, orchids, herbs, gardens, and grasslands
3	Bare land	Naturally occurring soils with no vegetation cover or above-ground cover within the study area.
4	Water bodies	River, permanent open water, lakes, ponds, canals, and Reservoirs

2.5Accuracy Assessment

This study used the confusion/error matrix to perform an accuracy evaluation in order to ascertain the correctness and reliability of the land use and land cover data. As noted byHasmadi et al. (2009), evaluating the accuracy of image classification is a crucial phase in ascertaining the dependability of the outcomes acquired from the classification procedure. Anderson (1997) said

that when identifying land cover classes from remotely sensed data, at least 85% interpretation accuracy should be achieved.To calculate for the producer accuracy, user accuracy, and overall accuracy Equation (1) was used.

$$\text{Overall Accuracy (\%)} = \frac{\text{Total Number of correctly classified samples}}{\text{Total number of samples}} \times 100 \quad \ldots (1)$$

$$\text{Kappa} = \frac{P(a) - P(e)}{1 - P(e)} \quad \ldots(2)$$

Where,

P(a) is the relative observed agreement

P(e) is the hypothetical probability of chance agreement.

2.6 Land Surface Temperature Retrieval

Using the Single Channel Algorithm (SCA) to get land surface temperature (LST) from thermal bands of a satellite image is a complex undertaking that requires a number of steps. The Landsat 8 OLI imageries were utilized for this purpose.

2.6.1 Conversion of Digital Numbers to Top-of-Atmosphere (TOA)

The conversion of spectral radiance digital numbers (DNs), which are contained in the thermal data of the Landsat sensor, into radiance units is the first step in calculating the Landsat surface temperature (LST). This method gives a way to represent pixels that haven't been calibrated yet. The following equation is used:

$$L\lambda = ML \times Q_{cal} + AL - O_i \quad \ldots (3)$$

Where,

$L\lambda$ is the TOA spectral radiance in Watts/ (m^2.sr. µm)

ML is the band-specific multiplying rescale factor in the metadata

AL is the band-specific additive rescaling factor in the metadata

Q_{cal} is the calibrated and quantized pixel values (DN),

O_i represents the offsets supplied by USGS for the TIRS band calibration (Sobrino*et al*., 2004).

2.6.2 Conversion of Radiance to Brightness Temperature (BT)

It is necessary to convert the converted TOA to brightness temperature (BT) by eliminating the atmospheric impacts in the thermal zone (Barsi et al., 2005). This is computed using pre-launch calibration constants and the assumption of unity emissivity. In order to update the radiant temperature, add absolute zero (around −273.15 ◦C). To achieve this, the following equation and the thermal constants listed in the metadata file were used.

$$BT = \frac{K2}{Ln\,(K1/\,L\lambda + 1)} - 273.15 \qquad \ldots(4)$$

Where,

Lλ is the TOA spectral radiance

K1 is the Band 10 constant band-specific thermal conversions from the metadata

K2 is the Band 11 constant band-specific thermal conversions from the metadata.

2.6.3 Calculating of Normalized Difference Vegetative Index (NDVI)

Due to its dependence on variables like land surface emissivity and proportional vegetative index (PV), the NDVI is a crucial component in the computation of land surface temperature (LST). The NDVI was computed using the following equation:

$$NDVI = \frac{NIR - Red}{NIR + Red} \qquad \ldots (5)$$

Where,

NIR is near-infrared band

Red is red band.

For this study, Landsat 8 OLI data was utilized and the near infrared is Band 5 while Red is Band 4.

2.6.4 Calculating Proportionate Vegetation Index (PV)

According to Sobrino*et al.,* (2004), the PV is the vegetation proportion viewed by derived using the following equation:

$$PV = \frac{NDV - NDVI\ min}{NDVI\ max - NDVI\ min} \quad \ldots (6)$$

Where,

NDVI max is for vegetation and NDVI min is for bare ground

2.6.5 Calculating Land Surface Emissivity (LSE)

An essential component in determining the LST is the land surface emissivity (Darren et al., 2020). This proportionality factor represents the efficiency of transmitting thermal energy across the surface into the atmosphere and scales blackbody radiance (Planck's law) to predict emitted radiance. The LSE can be calculated using the following equation

$$LSE = \varepsilon S \times (1 - Pv) + (\varepsilon V \times Pv) \quad \ldots(7)$$

Where,

εV and εS are the vegetation and soil emissivity, respectively

Pv is the proportionate vegetation index

For this study, the emissivity constants of Band 10 of Landsat 8 OLI was used which are εS = 0.971 and εV = 0.987 respectively.

2.6.6 Calculating Land Surface Temperature (LST)

$$LST = \frac{BT}{1 + \left(\frac{BT}{\rho}\right) Ln\ LSE} \quad \ldots(8)$$

Where,

BT is at-sensor brightness temperature,

$\rho = h \times c/\sigma = 1.438 \times 10^{-2}$ mK, and it is further converted to μm units

Furthermore, h is Planck's constant (6.626 × 10-34 Js), σ is the Boltzmann constant (1.38 × 10^{-}23 J/K) and c is the velocity of light (2.998 × 108 m/s) (Avdan and Jovanovska, 2016).

2.7LULC Types Impacts Analysis on LST

To ascertain the effects of LULC types on LST of Imo State, the data of LULC and LST were combined. This was accomplished using the data integration method in ArcGIS.

3.0 Results and Discussion

3.1 Classification Results

The results of the LULC Analysis using supervised classification method from 2013 to 2023 are presented in Fig 3 and Table 3 respectively.

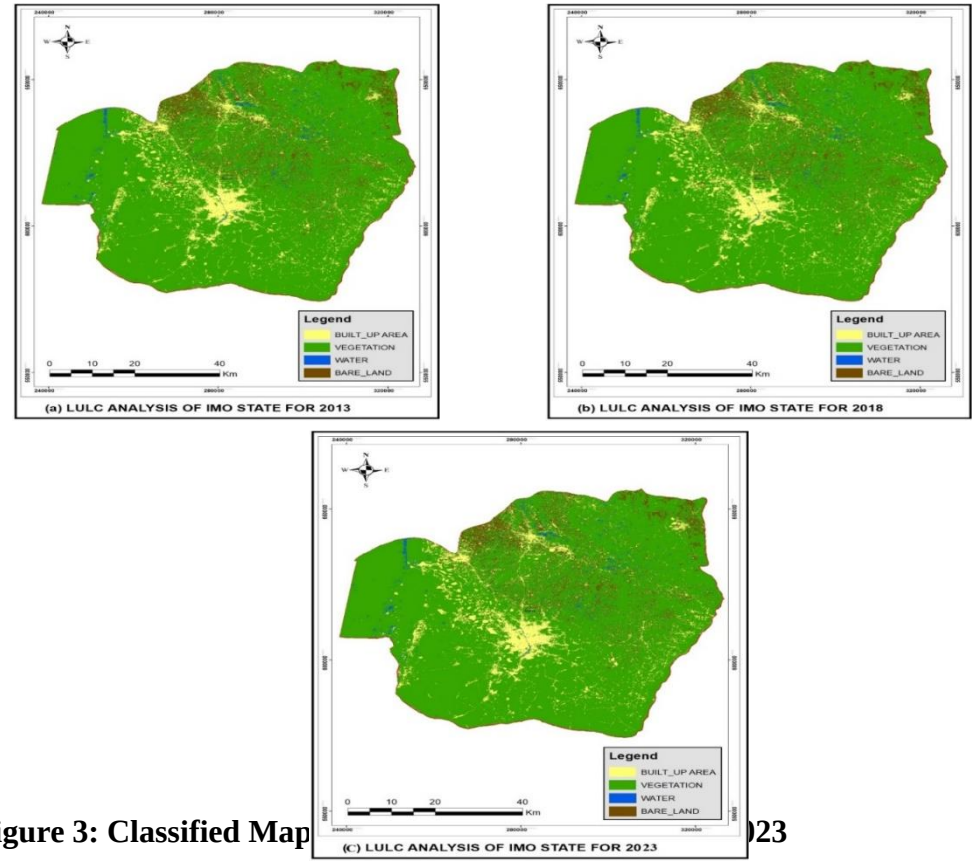

Figure 3: Classified Map 023

Table 4: Classification Results

Year	Built-up Areas (Sq.Km)	Vegetation (Sq.Km)	Bare Lands (Sq.Km)	Water Bodies (Sq.Km)
2013	1237.611(22.38%)	4017.536 (72.65%)	115.577 (2.09%)	159.176 (2.88%)
2018	1336.045 (24.16%)	3934.033(71.14%)	126.084 (2.28%)	133.826 (2.42%)
2023	1386.368 (25.07%)	3875.415 (70.08%)	155.946 (2.82%)	112.259 (2.03%)

From the results as shown in Fig 3 and Table 3, vegetation was the highest landusewith an area of 4017.536Sq. Km(72.65%), followed by built-up areas with 1237.611Sq. Km (22.38%), bare lands with 115.577Sq. Km (2.09%) and water bodies with 159.176Sq. Km (2.88%)in the year 2013. In 2018, the highest landuse was vegetation with an area of 3934.033Sq. Km (71.14%), followed by built-up areaswith 1336.045Sq. Km (24.16%),the bare lands and water bodies occupies 126.084Sq. Km (2.28%)and 133.826Sq. Km (2.42%) respectively. Furthermore, in 2023, vegetation occupied was the highest landusewith an area of 3875.415Sq. Km (70.08%), followed by built-up areas 1386.368Sq. Km (25.07%), the bare lands and water bodies occupies 155.946Sq. Km (2.82%) and 112.259Sq. Km (2.03%) respectively.

3.2 Classification Accuracy Assessment

The accuracy and dependability of the study's land use and land cover analysis were assessed using the confusion/error matrix. Tables 4, 5, and 6 shows the accuracy assessment findings, accordingly.

Table 4: Classification Accuracy Assessment for 2013

LanduseClasses	Built- up	Vegetation	Bare Lands	Water bodies	Total	User's Acc. (%)
Built- up	76	0	3	0	79	96.20
Vegetation	0	56	0	1	57	98.25
Bare Lands	4	0	68	0	72	94.44
Water bodies	0	3	0	63	66	95.45
Total	80	59	71	64	274	

Producer's Acc. (%)	95.00	94.92	95.77	98.44
Overall Acc. (%)	95.99			
Kappa Coefficient	0.96			

Table 5: Classification Accuracy Assessment for 2018

LanduseClasses	Built- up	Vegetation	Bare Lands	Water bodies	Total	User's Acc. (%)
Built- up	74	0	2	0	76	97.37
Vegetation	0	54	0	3	57	94.74
Bare Lands	2	0	61	0	63	96.83
Water bodies	0	2	0	59	61	96.72
Total	76	56	63	62	257	
Producer's Acc. (%)	97.37	96.43	96.83	95.16		
Overall Acc. (%)	96.50					
Kappa Coefficient	0.97					

Table 6: Classification Accuracy Assessment for 2023

LanduseClasses	Built- up	Vegetation	Bare Lands	Water bodies	Total	User's Acc. (%)
Built- up	76	0	1	0	77	98.70
Vegetation	0	56	0	1	57	98.25
Bare Lands	1	0	59	0	60	98.33
Water bodies	0	2	0	63	65	96.92
Total	77	58	60	64	259	
Producer's Acc. (%)	98.70	96.55	98.33	98.44		
Overall Acc. (%)	98.07					

Kappa Coefficient 0.98

3.3 Land Surface Temperature (LST) Results

The Single Channel Algorithm (SCA) was used to get the LST. Utilizing the study's Landsat 8 OLI imagery, the LST was successfully extracted using the Raster Calculator Tools in the ArcGIS software suite. Fig. 4 presents the findings.

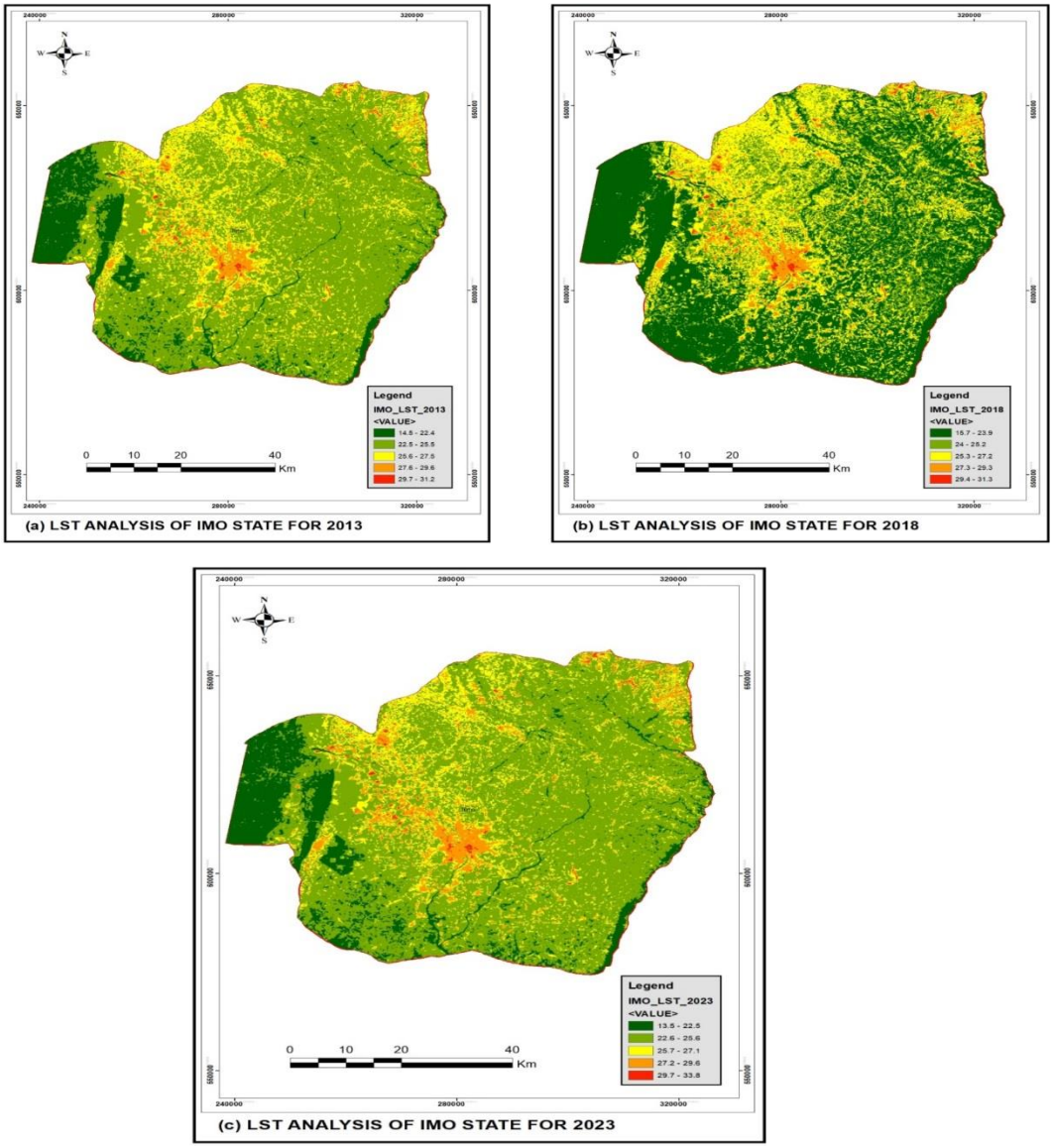

Figure 4: LST Maps of (a) 2013, (b) 2018, and (c) 2023

The results as shown in Fig 4, in 2013 it were observed that the LST range is from 14.5◦C to 31.2◦C. The lowest LST was 14.5◦C while the highest LST was 31.2◦C. In 2018, the LST range is from 15.7◦C to 31.3◦C. The lowest LST was 15.7◦C while the highest LST was 31.3◦Cand in 2024, the LST range is from 13.5◦C to 33.8◦C. The lowest LST was 13.5◦C while the highest LST was 33.8◦C.

3.4 Impact of LULC Types on LST Results

The different LULC types were analyzed to determine their various impacts on LST. The results of the analysis were presented in Table 7.

Table 7: Impact of LULC Types on LST of Imo State from 2013 to 2023

Year	Built-up	Vegetation	Bare Land	Water
	LST	LST	LST	LST
2013	22.38%	72.65%	2.09%	2.88%
	27.5◦C-31.2◦C	22.5◦C-25.4◦C	25.5◦C-27.4◦C	14.5◦C-22.4◦C
2018	24.16%	71.14%	2.28%	2.42%
	27.2◦C-31.3◦C	23.9◦C-27.1◦C	23.9◦C-25.2◦C	15.7◦C-23.8◦C
2023	25.07%	70.08%	2.82%	2.03%
	27.1◦C-33.8◦C	22.6◦C-25.6◦C	25.7◦C-27.0◦C	13.5◦C-22.5◦C

From the results in Table 7, in 2013, it was observed thatbuilt-up areas had the highest LST range, with an average LST range of 27.5◦C to 31.2◦C. Bare lands had the second highest LST range, at 25.5◦C to 27.4◦C. Vegetation had the third highest LST range, at 22.5◦C to 25.4◦C, and water had the lowest, at 14.5◦C to 22.4◦C. In 2018, the highest LST range was found in built-up areas, where it averaged 27.2◦C to 31.3◦C; the second highest LST range was found in bare lands, where it was 23.9◦C to 25.2◦C; the third highest LST range was found in vegetation, where it was 23.9◦C to 27.1◦C; and the lowest waswater with an LST range of 15.7◦C to 23.8◦C.Furthermore, in 2023, the highest LST ranges were found in built-up areas, with average LST ranges of 27.1◦C to 33.8◦C;

bare lands had the second-highest LST ranges, at 25.7◦C to 27.0◦C; vegetation had the third-highest LST ranges, at 22.6◦C to 25.6◦C; and water had the lowest, at 13.5◦C to 22.5◦C.

4. Conclusion

This study investigated into how different Land Use and Land Cover (LULC) types affected Land Surface Temperature (LST) in Imo State. The results suggest that because of the biophysical properties of the land surfaces, LULC has a considerable impact on LST values. It is suggested that incorporating vegetation into urban areas on a regular basis can assist maintain a cooler urban thermal environment since both vegetation and water bodies reduce surface temperatures. The greatest LST variations were found between water bodies and vegetation, but moderate LST differences were found between bare lands and vegetation as well as between barren land and built-up regions. The study also revealed that the highest LSTsoccur in the state's capital Owerri and also Mgbidi Town.

The study recommend the following:

i. In order to lower the high LST in built-up and urban areas, green spaces and greeneries should be established in the study area.

iii. A sustainable state development strategy to manage agricultural and grazing operations, among other anthropogenic activities should be established.

References

Anderson, J.R.(1997). Land use classification schemes used in selected recent geographic applications of remote sensing, *Photogrammetric Engineering*, 37 (4) 379–387.

Avdan, U., andJovanovska, G. (2016). Algorithm for Automated Mapping of Land Surface Temperature Using LANDSAT 8 Satellite Data.*Journal of Sensors*.

Barsi, J. A., Schott, J. R., Palluconi, F. D., and Hook, S. J. (2005). Validation of a web-based Atmospheric correction tool for single thermal band instruments (Conference session). Proceedings SPIE, 58820 E, Bellingham, WA, p. 7.

Darren, H. J. A., Mohd, H. I. and Farrah, M. M. (2020).Land Use/Land Cover Changes and the Relationship with Land Surface Temperature Using Landsat and MODIS Imageries in Cameron Highlands, Malaysia. Land 2020

Fonseka, H.P.U., Zhang, H., Sun, Y., Su, H., Lin, H., and Lin, Y. (2019). Urbanization and its impacts on land surface temperature in Colombo metropolitan area, Sri Lanka, from 1988 to 2016. Remote Sensing, 11 (8, 957), 18 pp

Hasmadi, M.,Pakhriazad, H.Z. andShahrin, M.F. (2009). Evaluating supervised and unsupervised techniques for land cover mapping using remote sensing data, *Malaysian Journal of Social Space*, 5 (1) 1–10

Hossain, M.S., Arshad, M., Qian, L., Kächele, H., Khan, I., Islam, M.D.I, Mahboob, M.G., 2020. Climate change impacts on farmland value in Bangladesh. *Ecological Indication*.112, 106181.

Luck, M., Wu, J., 2002. A gradient analysis of urban landscape pattern: a case study from the Phoenix metropolitan region, Arizona, USA. *Landscape Ecology*, 17, 327–339.

Mallick, J., Kant, Y., & Bharat, B. (2008). Estimation of land surface temperature over Delhi using Landsat-7 ETM+. *Journal of Indian Geophysical Union*, 131-140.

Sobrino, J.A., Munoz, J.C.J. and Leonardo, P. (2004). Land surface temperature retrieval from LANDSAT TM 5.*Remote Sensing of Environment*, 434 – 440

Tan, K.C., San Lim, H., MatJafri, M.Z. and Abdullah, K. (2010). Landsat data to evaluate urban expansion and determine land use/land cover changes in Penang Island, Malaysia. *Environmental Earth Science*.60, 1509–1521.

Weng, Q. (2001). A remote sensing-GIS evaluation of urban expansion and its impact on surface temperature in the Zhujiang Delta, China. *International Journal of Remote Sensing*, 22.